Size-dependent Effect of MgAl-Layered Double Hydroxides Derived from Mg(OH)2 on Thermal Stability of Poly(vinyl chloride)

Yixuan Guo, Qian Zhang, Weiliang Tian, Leroux Fabrice, Pinggui Tang, Dianqing Li, Yongjun Feng

Size-dependent Effect of MgAl-Layered Double Hydroxides Derived from $Mg(OH)_2$ on Thermal Stability of Poly(vinyl chloride)

Yixuan Guo,[1] Qian Zhang,[1] Qianqing Hu,[1] Weiliang Tian,[2,*] Fabrice Leroux,[3] Pinggui Tang,[1] Dianqing Li,[1] Yongjun Feng [1,2,*]

[1]State Key Laboratory of Chemical Resource Engineering, Beijing Engineering Center for Hierarchical Catalysts, College of Chemistry, Beijing University of Chemical Technology, No. 15 Beisanhuan East Road, Beijing 100029, China.

[2]Key Laboratory of Chemical Engineering in South Xinjiang, College of Life Science, Tarim University, Alar 843300, P. R. China.

[3]Université Clermont Auvergne, Institut de Chimie de Clermont-Ferrand ICCF, UMR-CNRS 6296, F 63171 Aubière, France.

*Corresponding authors: twllong@126.com (W. L. Tian), yjfeng@mail.buct.edu.cn (Y. J. Feng)

Abstract: Developing green thermal stabilizer for poly(vinyl chloride) (PVC) today is a great challenge for materials as polymer filler. Here, the "salt-oxide/hydroxide" route in mild conditions is used to fabricate a series of Mg_2Al-CO_3-LDH samples from $Mg(OH)_2$ precursors with different average particle sizes from 202 ± 10 nm to 334 ± 13 nm. A linear correlation is observed for the lateral size of the platelets between Mg_2Al-CO_3-LDH samples and their associated $Mg(OH)_2$ precursors. After surface-organo-modification (SOM), organophilic Mg_2Al-CO_3-LDH samples are found to be highly dispersed into PVC and investigated as environment-friendly thermal stabilizers. From the static/dynamic tests, the performances are strongly enhanced and related to the particle size of the LDH stabilizer, with the yellowish color aspect appearing later than for the commercial HT-3/PVC. Among the LDH series, the platelets with an average particle lateral size of about 220 ± 10 nm perform the best for the thermal stability for PVC polymer. Among the series, the corresponding PVC composite film presents comparatively the minimum color value in static/dynamic discoloration test, exhibiting the longer ignition time for proton initial release as well as the longer stability time in dehydrochlorination test. It underlines that the salt-oxide/hydroxide route is an efficient and environmentally friendly process in producing high-performance green LDH stabilizer for PVC.

Keywords: Layered double hydroxides, green route, poly(vinyl chloride) (PVC), particle size, thermal stabilizer

1. Introduction

Poly(vinyl chloride) (PVC) is the third-most widely used polymer around the world, and largely applied in various fields such as construction, chemical, and packaging, electric and electronic products, and so forth [1-3]. In addition, the statistics anticipate a global demand for PVC to reach 46.3 million tons in 2019 and to continuously increase [4]. However, PVC resins

have a poor thermal stability: this is mostly due to the fact that particularly, its processing is occurring at temperature higher than the dehydrochlorination and thermal degradation temperature thus making it highly fragile. Therefore, a thermal stabilizer is usually required to add during the processing of PVC to enhance its thermal stability as well as to retard its thermal degradation [5]. Hitherto, various thermal stabilizers have been developed and generally used in the market, for instance, lead salts, metal soaps, organotin, and other organic composites [6]. However, most of them are toxic towards human being in a certain degree. Indeed, the lead salts have been strictly limited by the European Union's RoHS and REACH directives. Usually, more than one organic stabilizer is needed to stabilize thermally PVC, moreover they are mostly hazardous chemicals. To challenge high-performance and environment-friendly thermal stabilizers for PVC, the layered double hydroxides (LDH) appear promising.

Indeed, for the last forty years and since the first patent (US4299759) in the 1980's [7], LDH–type materials have drawn more and more attention as a potential "green" thermal stabilizer for PVC [8-11]. The thermal stability mechanism of LDHs is found to proceed in two ways: one is the anion-exchange reaction between Cl^- in HCl from PVC and CO_3^{2-} into the LDH interlayer region, and the other is the possible neutralization reaction between HCl produced during PVC degradation and the alkaline LDH layers [12]. The first is to trap the aggressive Cl^- anions, LDH host is acting as a scavenger, while in the second LDH is dissolved under pH, thus buffering the medium. Most interestingly, LDH filler is acting under pH and chloride anions concentration stimuli, and silent otherwise. This aspect of a dormant load until reacting when necessary is reminiscent of LDH filler used in polymer coatings to inhibit corrosion phenomenon occurring onto metal substrate [13]. In decades, the effects of different Mg/Al ratios, intralayer cations and interlayer anions substitution of LDHs on the thermal stability property of PVC have been

investigated in detail in the literature [9-11,14], but t it is here beyond the scope of the study. Since the thermal stability performance of the LDH/PVC composite should also depend on the state of dispersion of the LDH particles within the composite, the focus is on their particle size and size distribution [15-20]. Usually, LDH-type materials were prepared by the so-called coprecipitation from the reaction between metal salts in alkaline medium as reported in academy as well as in industry. However, in this route, huge amount of water is produced in the washing steps that makes irrelevant in terms of sustainable development at any large scale-up [21-25]. More recently, the so-called "green" synthesis route has been developed using mixture between metal oxide and hydroxide or salt-oxide and hydroxide to reduce drastically the amount of water used during the washing step [26-30]. However, the former is difficult to yield LDH platelets suitable as thermal stabilizer for transparent PVC due to their sizes too large beyond micrometer [31], while the latter is not reported to fabricate LDH filler as PVC stabilizer so far [20]. Therefore, there is still a great challenge to fabricate high-performance and environment-friendly LDH thermal stabilizer for PVC composites.

In this work, a series of Mg_2Al-CO_3-LDH samples with different particle sizes was first prepared by the salt-hydroxide route using $Mg(OH)_2$, $Al(NO_3)_3 \cdot 9H_2O$, and light magnesium carbonate (LMC) as the feeding materials and by adjusting the particle size of $Mg(OH)_2$ precursor. In a second step, the LDH filler was organo-modified onto the platelets, leading to a surface compatibilized hybrid structure so called hereafter surface organo-modified LDH, SOM-LDH, towards polymer. Finally, the PVC/SOM-LDH composites were melt-blended in an open twin-wheel mill, and subsequently investigated for their thermal stability performance as a function of the LDH particle size.

2. Experimental section

2.1. Chemicals

$Mg(NO_3)_2 \cdot 6H_2O$, NaOH, $Al(NO_3)_3 \cdot 9H_2O$, calcium stearate ($Ca(st)_2$), and zinc stearate ($Zn(st)_2$) were purchased from Tianjin Fuchen Chemical Reagents Factory. Dioctyl phthalate (DOP), light magnesium carbonate (LMC) and stearic acid were obtained from Beijing Tongguang Fine Chemicals Co., Ltd. All the reagents were A.R. grade and directly used without further purification. PVC (SG-5 with average polymerization degree of 1000-1100) and the commercial Mg_2Al-CO_3-LDH (HT-3) were supplied, respectively, from Xinjiang Tianye Co., Ltd. and Kyowa Chemical Industries of Japan. All the water used was deionized.

2.2. Synthesis of Mg_2Al-CO_3-LDH from $Mg(OH)_2$ precursors

A series of Mg_2Al-CO_3-LDH samples were prepared in the salt-hydroxide route using the obtained $Mg(OH)_2$, $Al(NO_3)_3 \cdot 9H_2O$ and LMC as the feeding materials. The synthesis method of $Mg(OH)_2$ is shown in Supporting Information (SI), and the prepared $Mg(OH)_2$ samples were marked as $Mg(OH)_2$-aging time, for example $Mg(OH)_2$-1 h was for the $Mg(OH)_2$ aged at 90 °C for 1 h in the autoclave. For LDH-b, for instance, the slurry of $Mg(OH)_2$-1 h (123.40 g, solid content =3.26 %, 0.069 mol) and 1.46 g (0.003 mol) of LMC were dispersed in 130 mL of water to form a magnesium suspension under stirring, and 9.00 g (0.024 mol) of $Al(NO_3)_3 \cdot 9H_2O$ was dissolved in 50 mL of water to form a Al^{3+}-containing solution, which was added into the magnesium suspension by injector at the speed of 25 mL/h. Then the resulting suspension was transferred to a 500 mL four-neck flask and aged at 90 °C for 8 h at stirring speed of 500 r/min. Finally, the precipitate was centrifuged and washed with water for 1 cycle. The obtained slurry was separated in two parts: one was for the preparation of the organic-modified Mg_2Al-CO_3-LDH; and the other was for further physical characterization. The LDH samples were noted as LDH from a to g, corresponding to $Mg(OH)_2$ precursor from 0 h to 16 h.

2.3. Organic modification of Mg_2Al-CO_3-LDH

In order to enhance the compatibility with the PVC, the LDH samples were further organic-modified by stearic acid as described in the literature [32-34]. For example, the LDH-b slurry (31.20 g, solid content = 18.7 %, 12 mmol) was dispersed in 500 mL of water (solid content < 2 %), and then transferred into a 1 L three-neck flask under mechanical stirring. Subsequently, 0.47 g (1.65 mmol) stearic acid was dissolved into 50 mL of hot water, and then placed into the above-mentioned flask when the reaction temperature reached 80 °C. The resulting slurry was reacted at 80 °C for 2 h. Finally, the suspension was centrifuged and dried at 60 °C overnight leading to the surface organic-modified LDH (SOM-LDH) powder.

2.4. Preparation of SOM-LDH/PVC composites

A series of SOM-LDH/PVC composites were prepared by melting blending method. Typically, in the static thermal stability test, 100.00 g PVC resin, 2.00 g stabilizers (0.44 g $Ca(st)_2$, 0.44 g $Zn(st)_2$ and 1.12 g SOM-LDHs) and 40.00 g DOP were mixed in a beaker. The above mixtures were plasticized in an open twin-wheel mill (BP-8175-A, Baopin Ltd., China) at 36 rpm and 30 rpm roll speeds at 185 °C for 4 min, and then the gap between the two rolls was controlled at 0.4 mm to prepare transparent SOM-LDH/PVC composite films, respectively. In the dynamic thermal stability test, a blend of 100.00 g PVC resin, 1.00 g stabilizers (0.22 g $Ca(st)_2$, 0.22 g $Zn(st)_2$ and 0.56 g SOM-LDHs) and 25.00 g DOP was pressed by twin-wheel mill at 190 °C to obtain transparent SOM-LDH/PVC film. In both cases, a neat PVC film was fabricated as the blank sample for comparison without a SOM-LDH filler using the same mass of other stabilizer and DOP as for SOM-LDH/PVC composite.

2.5. Characterization

Powder X-ray diffraction (PXRD) patterns were recorded on a Shimadzu XRD-6000 X-ray diffractometer (40 kV, 30 mA, Cu Ka radiation, λ= 0.154 nm) in the range from 3 ° to 70 °/2θ with a scan step of 10 °/min. The morphology and particle sizes of the samples were measured using a Zeiss Supra 55 scanning electron microscope (SEM) and the average particle size was calculated from more than 100 particles for each sample. Fourier transform infrared (FT-IR) spectra in the range of 4000 to 400 cm^{-1} with 2 cm^{-1} resolution were collected on a Bruker Vector 22 infrared spectrophotometer using the KBr disk method with a ratio of sample/KBr of 1: 100 and the film method for SOM-CO_3-LDH/PVC films. The thickness of the LDH samples and the dispersion of LDHs in PVC resins were estimated using a Digital Instruments Version 6.12 atomic force microscope (AFM). Differential scanning calorimeter (DSC) measurements were carried out in N_2 gas flow using a differential scanning calorimeter (DSC, METTLER TOLEDO, DSC1 STARe System).

2.6. Thermal stability tests of SOM-LDH/PVC composites

Static thermal stability of SOM-LDH/PVC composites were carried out by discoloration test and dehydrochlorination test.

Discoloration test: The discoloration test of PVC sheets was performed according to ISO 305: 1990-4 standard. The PVC film was approximately cut into 1×1 cm sheets and heated in temperature-controlled oven at 195 °C in air. Strips were removed from the oven every 10 min. The thermal stability of SOM-LDH/PVC composites was appraised by the color differences using a Konica Minolta CR-400 type automatic color difference meter. The △L*, △A* and △B* values were determined by this color meter. The CIE-L*A*B* values could be used to formulate a value for total change as △E by the equation:

$$\triangle E = \sqrt{(\triangle L^*)^2+(\triangle A^*)^2+(\triangle B^*)^2}$$

where △L*, △A* and △B* values represented the white (+) and black (-), red (+) and green (-), yellow (+) and blue (-), respectively. The △E value was chosen to describe the discoloration of PVC sheets. A low △E value corresponds to a low color difference.

Dehydrochlorination test: The release rate of HCl gas produced by the PVC decomposition was estimated by a dehydrochlorination test based on ISO 182-2: 1990-12 [14,35]. 1.50 g of transparent PVC film were cut into small pieces by 1×1 mm. Fig. S1 shows the schematic diagram of dehydrochlorination test equipment. The PVC pieces were placed in a 50 mL three-flask and immersed in an oil bath at 180 °C. The HCl gas released from PVC pieces was recovered into a 100 mL deionized water at room temperature by N_2 gas. The pH value of the water was measured by a Mettler Toledo FE28 type pH meter (resolution, 0.01) and the concentration of H^+ in water was calculated.

Dynamic thermal stability of SOM-LDH/PVC composites was performed by discoloration test under the plastication process with twin-wheel mill at 190 °C. A piece of PVC film was taken out of the twin-wheel mill every 5 min and their color changes were measured by the above-mentioned automatic color difference meter.

2.7. Transparent test of SOM-LDH/PVC composites

100.00 g PVC, 8.00 g stabilizers (1.76 g $Ca(st)_2$, 1.76 g $Zn(st)_2$ and 4.48 g LDHs), and 50.00 g DOP were placed into a beaker and mixed uniformly. The mixture was plasticized at 185 °C by twin-wheel mill, and then hot-pressed and moulded with a thickness of 5 mm using a plate vulcanizing machine.

3. Results and discussion

3.1. Structural analysis of Mg_2Al-CO_3-LDH

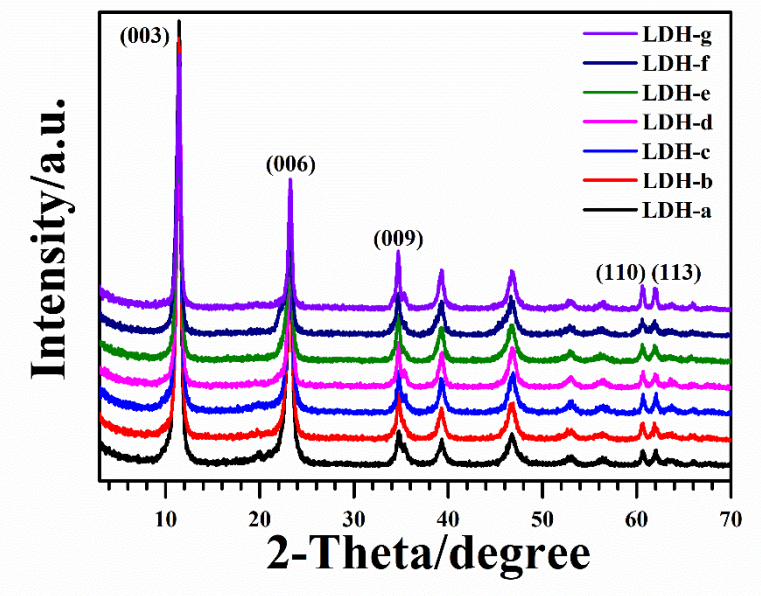

Fig. 1. PXRD patterns of Mg_2Al-CO_3-LDH samples (a-g) by the salt-hydroxide method from the corresponding $Mg(OH)_2$ precursors (0-16 h).

A series of Mg_2Al-CO_3-LDH samples were synthesized by the salt-hydroxide method using the above-prepared $Mg(OH)_2$ precursors, $Al(NO_3)_3$ and LMC as the feeding materials. Fig. 1 shows the PXRD patterns of the seven resulting Mg_2Al-CO_3-LDH samples. All the samples exhibit the typical PXRD patterns of LDH with the well-defined Bragg reflection peaks, e.g. (003), (006), (009) and (110) as marked in the graph. The basal *d*-spacing of Mg_2Al-CO_3-LDH is 0.78 nm calculated from the first three Bragg reflection peaks, which is in agreement with that of CO_3-type LDH reported in the literature [36].

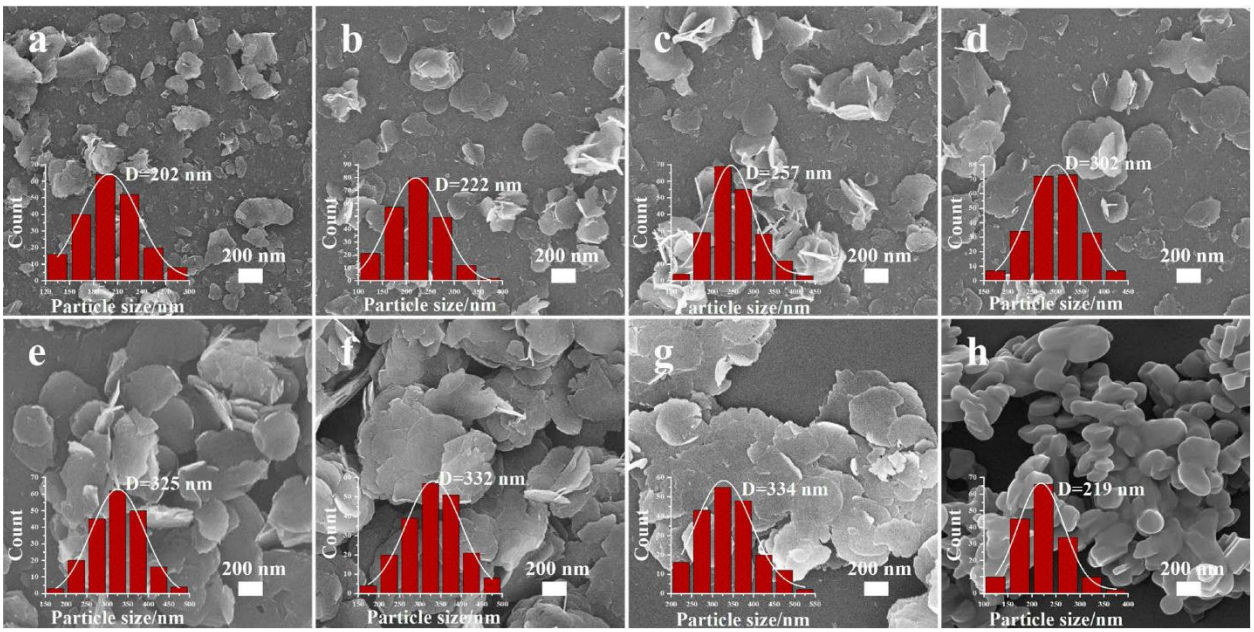

Fig. 2. SEM images of Mg_2Al-CO_3-LDH samples from the corresponding $Mg(OH)_2$ precursors (a-g) and commercial Mg_2Al-CO_3-LDH (HT-3) from Kyowa Chemical Industries of Japan (h).

Fig. 2 displays SEM images of the seven Mg_2Al-CO_3-LDH samples obtained by the salt-hydroxide method from different $Mg(OH)_2$ precursors compared to the commercial HT-3 sample from Kyowa Chemical Industries of Japan. The morphology of the as-made LDH samples and the HT-3 is for all platelet-like structures but with some slight differences: the as-made series exhibit a rather homogeneous hexagonal shape similar to $Mg(OH)_2$ precursor when lying flat on the substrate with the observation of thin-layer when exposed perpendicular. The reference HT-3 presents circular roundish aspect. Besides, Fig. 3a displays the particle size variation of $Mg(OH)_2$ and LDH extracted from Figs. S2 (Supporting information) and 2 as a function of the aging time of $Mg(OH)_2$. Interestingly, both series present a similar trend with a first rapid growth up to 8 h then to remain constant after. Indeed, Fig. 3b further demonstrates a close linear relationship in terms of particle size between LDHs and $Mg(OH)_2$ precursors. For example, the LDH platelets with the smaller particle lateral size of about 202 $\pm$ 10 nm were prepared from the smaller

particles of $Mg(OH)_2$ presenting a lateral size of 49 ± 5 nm, while the larger particle size of 334 ± 13 nm was from larger particles of $Mg(OH)_2$ of 176 ± 10 nm. This linear dependence may suggest a topochemical reaction between both materials, reminiscent of previous observation for the transformation from single to double layered hydroxides [37]. An in-situ characterization beyond the scope of the study will be necessary to unravel the reason of such lateral size dependence between the reactant and the reaction product, i.e., between the brucite and the LDH phase and why this LDH series mirrors that of the precursors. The above results suggest that it is an available and efficient route to prepare LDHs with different particle sizes by controlling that of $Mg(OH)_2$ precursor employed in the salt-hydroxide route. The particle size of HT-3 is 219 nm, close to that of LDH when using $Mg(OH)_2$-1h. Interestingly, the AFM image and associated height profile in Fig. 3c, d show that the platelets thickness of LDH-b sample is ca. 3.5 nm consisting of ca. 4 layers of LDH nanosheets, which is much thinner than ca. 24 nm measured for HT-3 (Fig. 2h) and as usually obtained by the traditional coprecipitation [38,39]. Besides, all the samples from LDH-a to -g display a stacking of platelets of similar thickness, that is close to that observed from samples prepared by another green route using MgO, Al_2O_3 and $NaNO_3$ [40]. Intuitively, thinner LDH platelets should improve the dispersion state of the LDH particles into PVC, thus to be more exposed to the polymer chains and more efficient to capture HCl when PVC degrades [41-44]. Evidently, the lateral size may play a role as a barrier effect, the LDH platelets acting as a sacrificial reservoir in improving PVC stability.

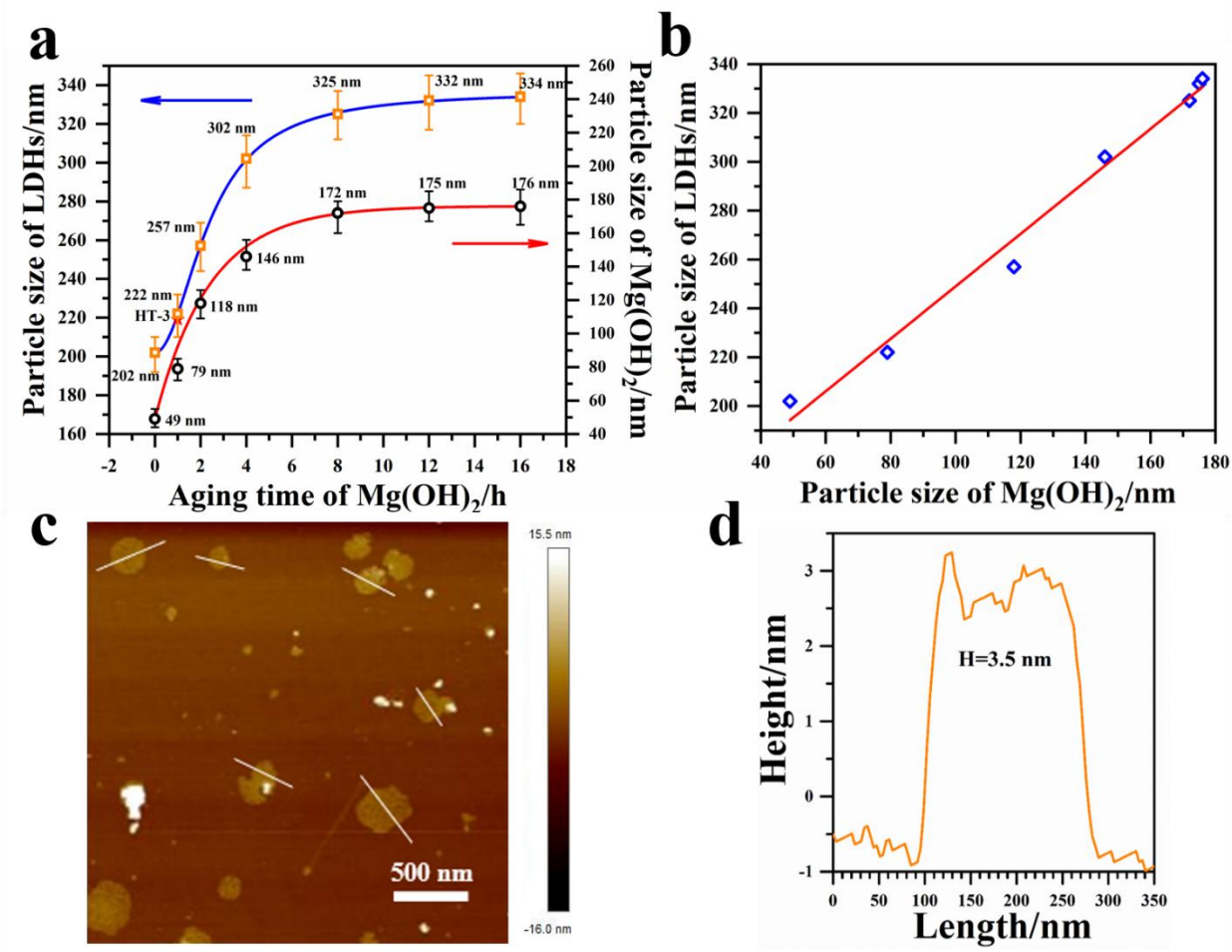

Fig. 3. (a) The particle size distribution of Mg_2Al-CO_3-LDH samples (blue curve) from the corresponding $Mg(OH)_2$ precursors (red curve); (b) the relationship of the particle size between Mg_2Al-CO_3-LDH and of $Mg(OH)_2$; AFM image of LDH-b (c) and their height profiles (d). The curves in a and b are guide for the eyes.

3.2. Structural analysis of SOM-LDH/PVC films

Fig. 4a displays the XRD patterns of LDH-b, SOM-LDH-b and SOM-LDH-b/PVC film (using a loading rate as low as 1.12 wt. %) and the commercial HT-3. Prior to the preparation of SOM-LDH-b/PVC composite by a melting blending method, LDH-b particles were organically surface-modified by stearic acid. Obviously, the LDH-b exhibits after the surface treatment a

same PXRD pattern than that of LDH-b and HT-3, indicating that the organic modification does not change the crystalline structure of the LDH and is occurring in absence of intercalation process [45]. Fig. 4b depicts the FT-IR spectra of LDH-b, SOM- LDH-b, stearic acid and SOM-LDH-b/PVC films. All of them, LDH-b, SOM-LDH-b, and HT-3, present characteristic IR absorption bands of CO_3-LDHs: ca. 3469 cm^{-1} for the O-H stretching vibration, 1645 cm^{-1} for the H-O-H deformation vibration of interlayer water, and another at 448 cm^{-1} for the lattice vibration (Mg-O and Al-O) in the host sheet, at 1367 cm^{-1} for the C-O stretching vibration belonging to CO_3^{2-} ions in the interlayer region. In comparison, SOM-LDH-b spectrum presents another two absorption bands at 2921 and 2847 cm^{-1} for the C-H stretching vibration assigned to the stearic acid. It indicates that stearate anions were adsorbed onto the surface, this to improve the chemical compatibility between the SOM-LDH-b and PVC [46]. Here, FT-IR spectrum of HT-3 also shows the similar absorption bands for the C-H stretching vibration assigned to the hydrophobic part of surfactant usually used to organo-modify clay-type structure, suggesting that HT-3 is also surface organo-modified. In the case of SOM-LDH-b/PVC, strong absorption bands in the range of 2900-3000 cm^{-1} attributed to C-H stretching vibration belong to PVC chains, as for the neat PVC film that shows the other strong absorbances (no transmittance between 750 and 1250 cm^{-1}) are due to PVC vibration (Figs. S4 and S5). The presence of LDHs in the composites is difficult to detect either from the IR absorption band or Bragg reflections due to the small mass used for the LDH loading. However, the Mg (blue dot)/Al (red dot) element mapping by SEM as well as AFM images reveal a high dispersion state of SOM-LDH-b platelets into PVC as shown in Fig. 4c-f.

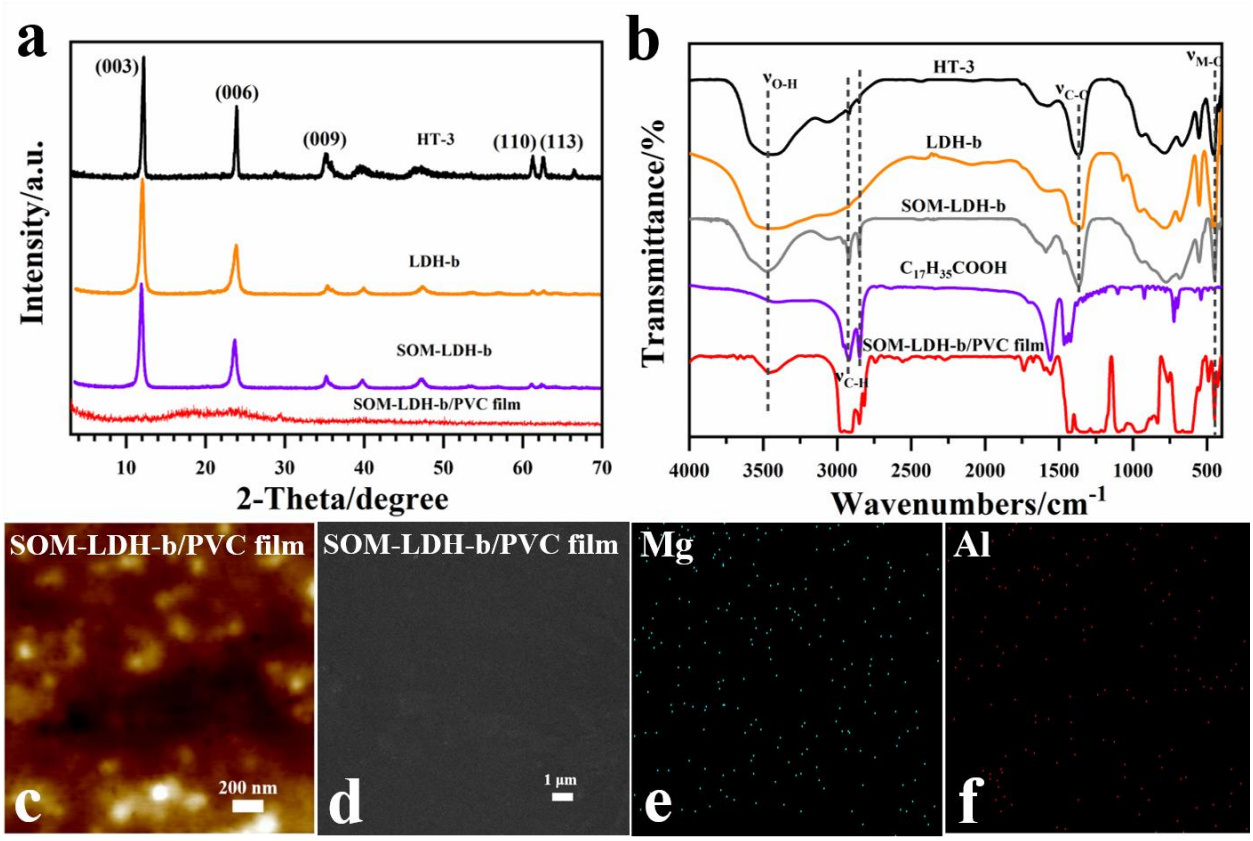

Fig. 4. (a) Powder X-ray diffraction patterns of LDH-b, SOM-LDH-b and SOM-LDH-b/PVC films; (b) FT-IR spectra of LDH-b, SOM-LDH-b, $C_{17}H_{35}COOH$ and SOM-LDH-b/PVC films; AFM (c) and SEM (d) images of SOM-LDH-b/PVC film; Mg element (e, blue), and Al element (f, red) mapping of SOM-LDH-b/PVC.

3.3. Thermal degradation behaviour of SOM-LDH/PVC composites

Fig. 5 shows the color change of SOM-LDH/PVC composite sheets in the static (a and b) and dynamics (c and d) thermal stability tests related to HT-3/PVC as the reference 47. In the static test, c.f., Fig. 5a, the initial whiteness for all the samples is similar, and then the LDH/PVC composite sheets turn from yellow to black with an increase of degradation time up to 80 min at 195 °C. Among these samples, the neat PVC sample (without addition of LDH) is blackened after 10 min, HT-3/PVC turns yellow from ca. 30 min and black after 40 min, while SOM-

LDH/PVC composites exhibit much longer thermal stability than PVC and HT-3/PVC. It suggests that the as-made LDH particles with ca. 4 layers should be dispersed easily in the polymer, thus more efficient to inhibit the thermal degradation of PVC, compared with HT-3 with ca. 30 layers, as reported in refs. 43 and 44. Interestingly, the thermal stability of SOM-LDH/PVC composites performs significantly lower by increasing the particle size. Quantitatively an increase from 202 ± 10 nm to 334 ± 13 nm shifts the time of a "yellow" appearance from 50 min to 30 min, however, they are all black after 80 min. In addition, Fig. 5b further demonstrates the color values of ΔE as a function of thermal degradation time. For example, SOM-LDH-b/PVC composite presents the minimum color value before turning black after 80 min, showing the best thermal stability among the series. In the dynamic test at 190 °C, Fig. 5c and d show that both SOM-LDH-a and -b/PVC exhibit the same thermal stability than that with HT-3/PVC, but in the first 30 min. The performance in the series after 45 min of test is directly ranked by the lateral size variation. One may note that the particle lateral size of the as-made SOM-stabilizers plays a key role in improving the thermal stability of PVC. As intuitively thought, an appropriate particle size of the filler favours its dispersion state into the composite, then being more exposed, it is more efficient to protect PVC from its degradation effect. To sum up, a small thickness and particle lateral size of LDH platelets have both significant influence on the thermal stability of LDH/PVC composites. The former is controlled during the "green" synthesis, the later can be tuned by reaction conditions.

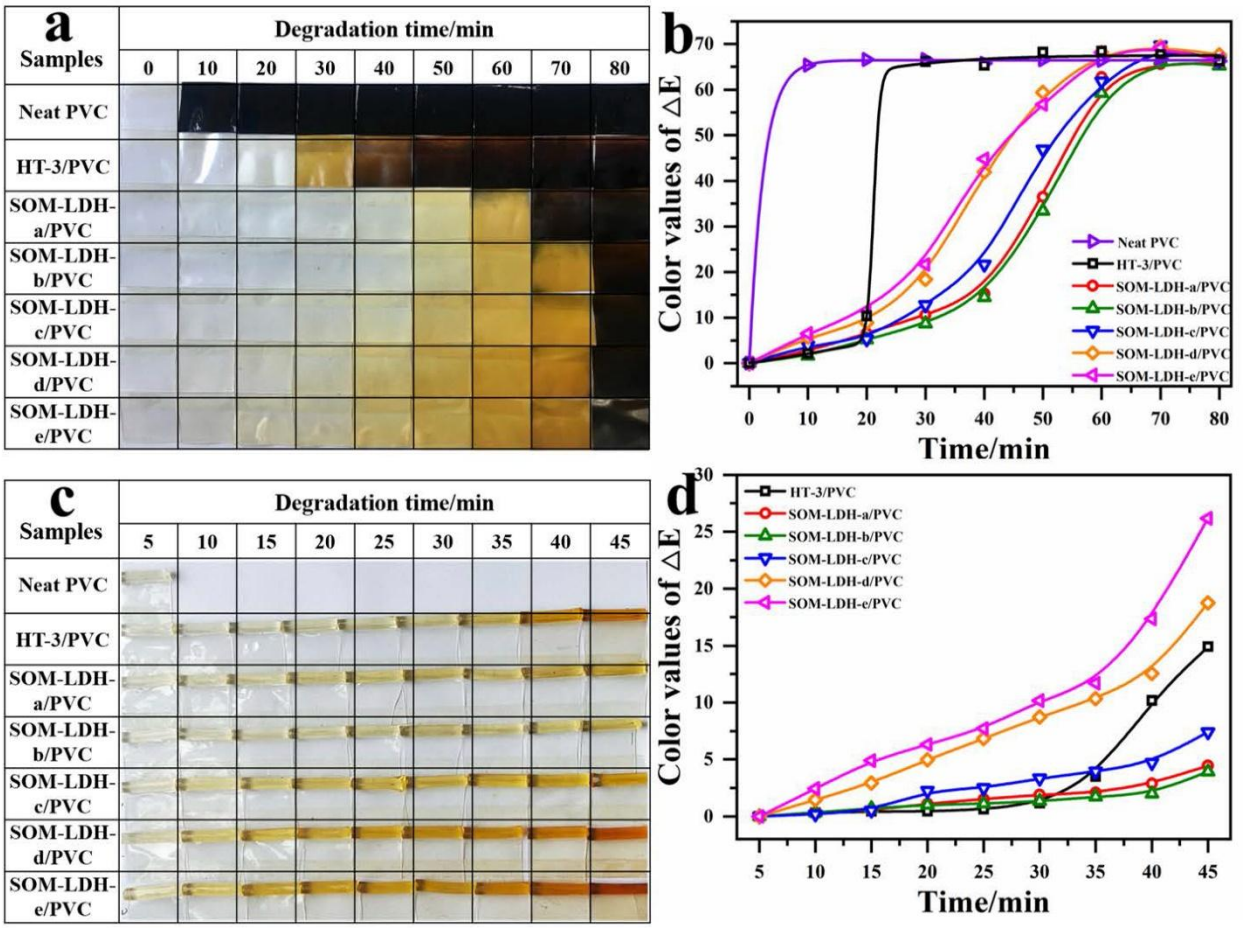

Fig. 5. Results of discoloration (a, c) and color values (b, d) of transparent PVC sheets at 195 °C and 190 °C in static (a, b) oven and dynamic (c, d) thermal stability tests. (Static test condition: baked in 195 °C oven, sheet composition: PVC(SG-5), 100 phr; Stablizer, 2 phr (LDHs 56%, CaZn 44%); DOP, 40 phr. Dynamic test condition: Test condition: plasticized in 190 °C double-roller blending rolls, sheet composition: PVC(SG-5), 100 phr; Stablizer, 1 phr (LDHs 56%, CaZn 44%); DOP, 25 phr).

During the thermal degradation process, a certain amount of HCl is released from PVC composites. Fig. 6a shows the concentration of protons as a function of the degradation time up to 240 min. In comparison, all the prepared SOM-LDH samples exhibit much higher capacity to

inhibit the HCl release from the PVC degradation than neat PVC or HT-3/PVC. The detailed results are scrutinized in terms of the ignition time (t_1) and the stability time (t_2) for deeper comparison (Fig. 6b). As reported in Ref. 45, t_1 is the time for the protons (H^+) to be released in solution and t_2 represents the time to reach a concentration of $2*10^{-3}$ mol/L. For example, t_1 is rather short of 9 min for neat PVC, and 30 min for HT-3/PVC, while much longer times are observed for the as-made SOM-LDH/PVC. Comparatively, t_1 ranks as follows: neat PVC < HT-3/PVC < SOM-LDH-a/PVC < SOM-LDH-e/PVC < SOM-LDH-d/PVC < SOM-LDH-c/PVC < SOM-LDH-b/PVC, and for t_2 neat PVC < HT-3/PVC < SOM-LDH-a/PVC <SOM-LDH-e/PVC < SOM-LDH-c/PVC < SOM-LDH-d/PVC <SOM-LDH-b/PVC. In addition, Fig. S6 displays first derivative curve of the HCl release rate as a function of time for the PVC samples according to data from Fig. 6a, showing that the ignition of HCl release for neat PVC is much faster than for PVC samples with filler as well as comparing the release rate from the relative intensity of the derivative curves. The observed trend agrees well with the discoloration test results in Fig. 5. In the series SOM-LDH/PVC composites, SOM-LDH-b/PVC exhibits the higher thermal stability associated to the longer ignition time t_1 of 114 min, and the longer stability time t_2 of 234 min. These above results demonstrate that the SOM-LDH is highly efficient to stabilize PVC in temperature, and to endow the polymer with the performance of interest for application.

Besides, transparency property is another important parameter for PVC product. Fig. 6c displays the photograph of 2 mm-thick films using composites LDH/PVC placed onto the printed school logo of Beijing University of Chemical Technology. One observes that the two PVC composites using either HT-3/PVC or SOM-LDH-b show a proper transparency, which most probably results from an appropriate particle size of the filler of ca. 220 $\pm$ 10 nm. Additionally, Fig. 6d displays the DSC curves of LDH/PVC composite films. The glass transition temperature

T_g is close to one measured for the neat PVC. It underlines that the addition of SOM-LDH filler has no significant influence on the PVC thermal behaviour or on its processability.

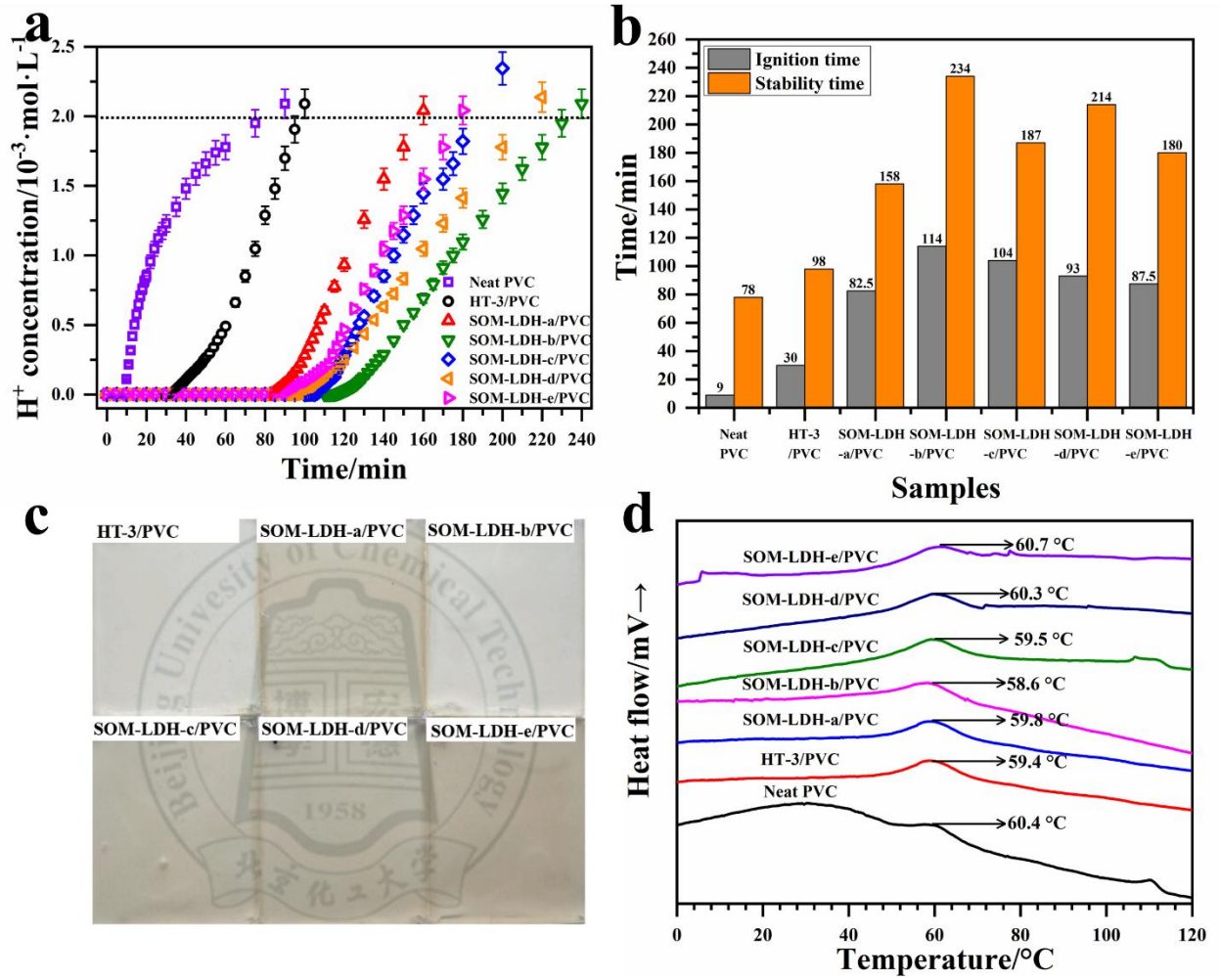

Fig, 6. (a) HCl release curves for the PVC samples heated at 180 °C; (b) The induction time and stability time of LDH/PVC sheets in dehydrochlorination test; (c) Transparency tests of LDH/PVC sheets. (d) DSC curves of LDH/PVC sheets.

4. Conclusions

In this work, the "salt-oxide/hydroxide" route in mild conditions is adopted to fabricate a series of Mg_2Al-CO_3-LDH samples with different particle sizes from 202 ± 10 nm to 334 ± 13 nm from $Mg(OH)_2$ precursor that is prepared by the SNAS method. The prepared Mg_2Al-CO_3-LDH samples are surface-organo-modified to render them organophilic and easily dispersible into PVC. As thermal stabilizer, the as-made series exhibits higher performance to inhibit the PVC thermal degradation when compared to commercially available LDH standard. Using static/dynamic tests, it is demonstrated that enhanced performances are strongly related to the particle size of the LDH stabilizer. Among the investigated LDH samples in our work, the better candidate comparatively into the series presents an average particle lateral size of about 220 ± 10 nm, close to the commercial standard. Computational modeling should be carried out to better understand such lateral size dependence against performance to further optimize PVC stability. In summary, the salt-oxide/hydroxide green route appears as transferable and environmentally friendly process to produce high-performance green LDH stabilizer for PVC.

Declaration of competing interest

The authors declare that they have no known competing financial interests or personal relationships that could have appeared to influence the work reported in this paper.

Acknowledgments

This work is supported by Natural Science Foundation of China (No. 21627813, 21761029, and U1707603), First Division Alar Science and Technology Plan Project in Xinjiang Corps (2019GJJ04), Program for Changjiang Scholars and Innovative Research Team in University (No. IRT1205) and Distinguished professor of Kunlun scholars in Tarim University.

References

[1] P. Jia, L. Hu, Q. Shang, R. Wang, M. Zhang, Y. Zhou, Self-plasticization of PVC materials via chemical modification of mannich base of cardanol butyl ether, ACS Sustain. Chem. Eng. 5 (2017) 6665-6673.

[2] F. Chiellini, M. Ferri, A. Morelli, L. Dipaola, G. Latini, Perspectives on alternatives to phthalate plasticized poly(vinyl chloride) in medical devices applications, Prog. Polym. Sci. 38 (2013) 1067-1088.

[3] N. Ahmad, A. Kausar, B. Muhammad, Perspectives on polyvinyl chloride and carbon nanofiller composite: a review, Polym-Plast Technol 55 (2016) 1076-1098.

[4] M. Bahls, O. Mieden, K. Mühlschlegel, F. Riedmiller, E. Vogel, Polyvinyl chloride (PVC), Kunststoffe international (2019) 26-29.

[5] J. Yu, L. Sun, C. Ma, Y. Qiao, H. Yao, Thermal degradation of PVC: a review, Waste Manag. 48 (2016) 300-314.

[6] D. Zhang, S. Yao, S. Li, J. Wang, Y. Yao, A novel La-containing additive for the long-term thermal stabilization of poly(vinyl chloride), Polym. Degrad. Stabil. 144 (2017) 187-194.

[7] S. Miyata, M. Kuroda, Method for inhibiting the thermal or ultraviolet degradation of thermoplastic resin and thermoplastic resin composition having stability to thermal or ultraviolet degradation, US4299759, 1981.

[8] X. Zhang, L. Zhou, H. Pi, S. Guo, J. Fu, Performance of layered double hydroxides intercalated by a UV stabilizer in accelerated weathering and thermal stabilization of PVC, Polym. Degrad. Stabil. 102 (2014) 204-211.

[89 J. Yan, Z. Yang, Intercalated hydrotalcite-like materials and their application as thermal stabilizers in poly(vinyl chloride), J. Appl. Polym. Sci. 134 (2017) 44896.

[10] R. Wen, Z. Yang, H. Chen, Y. Hu, J. Duan, Zn-Al-La hydrotalcite-like compounds as heating stabilizer in PVC resin, J. Rare Earth. 30 (2012) 895-902.

[11] S. Aisawaa, C. Nakadaa, H. Hiraharaa, N. Takahashib, E. Naritaa, Preparation of dipentaerythritol-combined layered double hydroxide particle and its thermostabilizing effect for polyvinyl chloride, Appl. Clay Sci. 180 (2019) 105205.

[12] X. Wen, Z. Yang, J. Yan, X. Xie, Green preparation and characterization of a novel heat stabilizer for poly(vinyl chloride)–hydrocalumites, RSC Adv. 5 (2015) 32020-32026.

[13] T. Stimpfling, P. Vialat, H. Hintze-Bruening, P. Keil, V. Shkirskiy, P. Volovitch, K. Ogle, F. Leroux, Amino acid interleaved layered double hydroxides as promising hybrid materials for AA2024 corrosion inhibition, Eur. J. Inorg. Chem. 2016 (2016) 2006-2016.

[14] F.J.W.J. Labuschagne, D. M. Molefe, W. W. Focke, I. v. d. Westhuizen, H. C. Wright, M. D. Royeppen, Heat stabilising flexible PVC with layered double hydroxide derivatives, Polym. Degrad. Stabil. 113 (2015) 46-54.

[15] C. Taviot-Guého, V. Prévot, C. Forano, G. Renaudin, C. Mousty, F. Leroux, Tailoring hybrid layered double hydroxides for the development of innovative applications, Adv. Funct. Mater. 28 (2018) 1703868.

[16] D. L. Schrijvers, F. Leroux, V. Verney, M. K. Patel, Ex-ante life cycle assessment of polymer nanocomposites using organo-modified layered double hydroxides for potential application in agricultural films, Green Chem. 16 (2014) 4969-4984.

[17] L. Qiu, Y. Gao, P. Lu, D. O'Hare, Q. Wang, Synthesis and properties of polypropylene/layered double hydroxide nanocomposites with different LDHs particle sizes, J. Appl. Polym. Sci. 135 (2018) 46204.

[18] B. Nagendra, C. V. S. Rosely, A. Leuteritz, U. Reuter, E. B. Gowd, Polypropylene/layered double hydroxide nanocomposites: influence of LDH intralayer metal constituents on the properties of polypropylene, ACS Omega 2 (2017) 20-31.

[19] B. Nagendra, K. Mohan, E. B. Gowd, Polypropylene/layered double hydroxide (LDH) nanocomposites: influence of LDH particle size on the crystallization behavior of polypropylene, ACS Appl. Mater. Inter. 7 (2015) 12399-12410.

[20] H. Liao, Y. Jia, L. Wang, Q. Yin, J. Han, X. Sun, M. Wei, Size effect of layered double hydroxide platelets on the crystallization behavior of isotactic polypropylene, ACS Omega 2 (2017) 4253-4260.

[21] F. L. Theiss, G. A. Ayoko, R. L. Frost, Synthesis of layered double hydroxides containing Mg^{2+}, Zn^{2+}, Ca^{2+} and Al^{3+} layer cations by co-precipitation methods—a review, Appl. Surf. Sci. 383 (2016) 200-213.

[22] K. Okamoto, N. Iyi, T. Sasaki, Factors affecting the crystal size of the MgAl-LDH (layered double hydroxide) prepared by using ammonia-releasing reagents, Appl. Clay Sci. 37 (2007) 23-31.

[23] Z. Gu, J. J. Atherton, Z. P. Xu, Hierarchical layered double hydroxide nanocomposites: structure, synthesis and applications, Chem. Commun. 51 (2015) 3024-3036.

[24] J-M. Oh, S-H. Hwang, J.-H. Choy, The effect of synthetic conditions on tailoring the size of

hydrotalcite particles, Solid State Ionics 151 (2002) 285-291.

[25] S. G. Intasa-Ard, K. J. Imwiset, S. Bureekaew, M. Ogawa, Mechanochemical methods for the preparation of intercalation compounds, from intercalation to the formation of layered double hydroxides, Dalton Trans. 47 (2018) 2896-2916.

[26] G. R. Williams, A. Clout, J. C. Burley, A kinetic and mechanistic study into the formation of the Cu-Cr layered double hydroxide, Phys. Chem. Chem. Phys. 15 (2013) 8616-8628.

[27] S.-L. Wang, C.-H. Lin, Y.-Y. Yan, M. K. Wang, Synthesis of Li/Al LDH using aluminum and LiOH, Appl. Clay Sci. 72 (2013) 191-195.

[28] J. Shin, C.-J. Choi, T.-H. Kim, J.-M. Oh, Phase transformation from brucite to highly crystalline layered double hydroxide through a combined dissolution–reprecipitation and substitution mechanism, Cryst. Growth Des. 18 (2018) 5398-5405.

[29] S. Nishimura, A. Takagaki, K. Ebitani, Characterization, synthesis and catalysis of hydrotalcite-related materials for highly efficient materials transformations, Green Chem. 15 (2013) 2026-2042.

[30] Z. Meng, Y. Zhang, Q. Zhang, X. Chen, L. Liu, S. Komarneni, F. Lv, Novel synthesis of layered double hydroxides (LDHs) from zinc hydroxide, Appl. Surf. Sci. 396 (2017) 799-803.

[31] F. J. W. J. Labuschagné, A. Wiid, H. P. Venter, B. R. Gevers, A. Leuteritz, Green synthesis of hydrotalcite from untreated magnesium oxide and aluminum hydroxide, Green Chem. Lett. Rev. 11 (2018) 18-28.

[32] M. Kotal, A. K. Bhowmick, Polymer nanocomposites from modified clays: recent advances and challenges, Prog. Polym. Sci. 51 (2015) 127-187.

[33] D. Basu, A. Das, K. W. Stöckelhuber, U. Wagenknecht, G. Heinrich, Advances in layered double hydroxide (LDH)-based elastomer composites, Prog. Polym. Sci. 39 (2014) 594-626.

[343] H. Zhang, Z. Yang, The effect of sodium stearate-modified hydrocalumite on the thermal stability of poly(vinyl chloride), J. Appl. Polym. Sci. 135 (2018) 45758.

[35] T. Dong, D. Li, Y. Li, W. Han, L. Zhang, G. Xie, J. Sunarso, S. Liu, Design and synthesis of polyol ester-based zinc metal alkoxides as a bi-functional thermal stabilizer for poly(vinyl chloride), Polym. Degrad. Stabil. 159 (2019) 125-132.

[36] Y. Guo, J. Wang, D. Li, P. Tang, F. Leroux, Y. Feng, Micrometer-sized dihydrogenphosphate-intercalated layered double hydroxides: synthesis, selective infrared absorption properties, and applications as agricultural films, Dalton Trans. 47 (2018) 3144-3154.

[37] T. Stimpfling, A. Langry, H. Hintze-Bruening, F. Leroux, In situ platelets formation into aqueous polymer colloids: the topochemical transformation from single to double layered hydroxide (LSH-LDH) uncovered, J. Colloid Inter. Sci. 462 (2016) 260-271.

[38] J. Yu, Q. Wang, D. O'Hare, L. Sun, Preparation of two dimensional layered double hydroxide nanosheets and their applications, Chem. Soc. Rev. 46 (2017) 5950-5974.

[39] Q. Wang, L. Chen, S. Guan, X. Zhang, B. Wang, X. Cao, Z. Yu, Y. He, D. G. Evans, J. Feng, D. Li, Ultrathin and vacancy-rich CoAl-layered double hydroxide/graphite oxide catalysts: promotional effect of cobalt vacancies and oxygen vacancies in alcohol oxidation, ACS Catal. 8 (2018) 3104-3115.

[40] F. Zhang, N. Du, S. Song, J. Liu, W. Hou, Mechano-hydrothermal synthesis of $Mg_2Al–NO_3$ layered double hydroxides, J. Solid State Chem. 206 (2013) 45-50.

[41] H. Yin, Z. Tang, Ultrathin two-dimensional layered metal hydroxides: an emerging platform for advanced catalysis, energy conversion and storage, Chem. Soc. Rev. 45 (2016) 4873-4891.

[42] Q. Wang, D. O'Hare, Recent advances in the synthesis and application of layered double hydroxide (LDH) nanosheets, Chem. Rev. 112 (2012) 4124-4155.

[43] Q. Zhang, Y. Guo, F. Leroux, P. Tang, D. Li, L. Wang, Y. Feng, An aqueous miscible organic (AMO) process for layered double hydroxides (LDHs) for the enhanced properties of polypropylene-LDH composites, New J. Chem. 44 (2020) 10119-10126.

[44] J.-H. Yang, W. Zhang, H. Ryu, J.-H. Lee, D.-H. Park, J. Y. Choi, A. Vinu, A. A. Elzatahryde, J.-H. Choy, Influence of anionic surface modifiers on the thermal stability and mechanical properties of layered double hydroxide/polypropylene nanocomposites, J. Mater. Chem. A 3 (2015) 22730-22738.

[45] F. Zhang, N. Du, S. Song, W. Hou, Mechano-hydrothermal synthesis of SDS intercalated LDH nanohybrids and their removal efficiency for 2,4-dichlorophenoxyacetic acid from aqueous solution, Mater. Chem. Phys. 152 (2015) 95-103.

[46] K. Sarita, K. Susheel, C. Annamaria, N. James, Y. H, R. K, Surface modification of inorganic nanoparticles for development of organic–inorganic nanocomposites—a review, Prog. Polym. Sci. 38 (2013) 1232-1261.

[47] Y. Shi, Y. Wang, B. Ma, M. Ma, S. Chen, X. Wang, Tensile properties, thermal stability, and the mechanism of PVC stabilized with zinc and calcium oxolinic complexes, J. Appl. Polym. Sci. 136 (2019) 47004.